

Motor driven microtubule shape fluctuations - force from within the lattice

Hervé Mohrbach¹ and Igor M. Kulić²

¹Laboratoire de Physique Moléculaire et des Collisions, Université Paul Verlaine - 57012 Metz, France

²School of Engineering and Applied Sciences, Harvard University, Massachusetts 02138, USA

(Dated: October 31, 2018)

We develop a general theory of microtubule (MT) deformations by molecular motors generating internal force doublets within the MT lattice. We describe two basic internal excitations, the S and V shape, and compare them with experimental observations from literature. We explain the special role of tubulin vacancies and the dramatic deformation amplifying effect observed for katanin acting at positions of defects. Experimentally observed shapes are used to determine the ratio of MT shear and stretch moduli ($\approx 6 \times 10^{-5}$) and to estimate the forces induced in the MT lattice by katanin (10's of pN). For many motors acting on a single MT we derive expressions for the end-to-end distance reduction and provide criteria for dominance of this new effect over thermal fluctuations. We conclude that molecular motors if acting cooperatively can "animate" MTs from within the lattice and induce slack even without cross-bridging to other structures, a scenario very much reminiscent of the motor driven axoneme.

PACS numbers: 87.15.-v 87.16.Ka 87.16.Nn

Microtubules are the stiffest cytoskeletal component and constitute the main routes for motor mediated intracellular cargo transport in higher organisms [1]. Understanding their physical properties is at the heart of many biological problems from cellular mechanics to information and material trafficking in the cell. Since the discovery of their high elastic anisotropy [2] it became increasingly clear that MTs are mechanically more complex than other semiflexible biofilaments. The high anisotropy has been impressively confirmed by thermal fluctuation analysis of beads attached to MTs of different lengths[3]. The emerging picture of the MT is that of an anisotropic fiber reinforced material [2, 3] with the tubulin protofilaments (PF) acting as strong fibers weakly linked with easily shearable lateral bonds. Remarkably this type of design is also found in higher structures like axonemes (constituting the backbone of flagella and cilia) where relatively inextensible MTs are held together with highly stretchable nexin connections [1]. This remarkable structural self-similarity of the two nested structures (MT and axoneme) indicates further analogies in the way they respond to external and internal forces. We explore here important consequences of MT geometry and elastic properties and show that motors acting on the MT surface can generate internal lattice strains sufficient to induce observable lateral and longitudinal deformations of the MT backbone.

In the following we describe a twist-free MT of length L consisting of N identical PFa with constant distance a and a circular cross section, Fig 1. Each PF, parametrized by the MT backbone arc length s has a position dependent displacement $u_k(s)$ from its equilibrium position, $k = 1, \dots, N$. The backbone shape is described by a curvature vector $\vec{\kappa}(s) = \frac{d}{ds}\vec{t}(s)$ with $\vec{t}(s)$ the bundle centerline tangent. The elastic properties of the MT are characterized by a PF bending stiffness $B = \frac{1}{64}\pi a^4 Y$ and compressional modulus $K_c = \frac{\pi}{4}a^2 Y$

with $Y \approx 0.1 - 1.5 GPa$ [2, 3] being the PF Young's modulus. Additionally there are shear elastic forces restoring the longitudinal displacement between the PFs governed by a very soft elastic shear modulus $K_s \approx 10^{-3} - 1 MPa$ [2, 3]. The elastic energy is given by

$$E_{MT} = \frac{1}{2} \sum_{k=1}^{k=N} \int_{-L/2}^{L/2} (B\vec{\kappa}^2 + K_c u_k'^2 + K_s \Delta_k^2) ds \quad (1)$$

with the first term being the bending energy, the second the PF compression and the third describing the relative shear energy between the neighboring PFs. The shear displacement Δ_k is related to the difference of PF displacements $u_k - u_{k-1}$ and a curvature induced additional displacement via

$$\Delta_k(s) = u_k(s) - u_{k-1}(s) + \int_{-L/2}^s \vec{\kappa}(s') \cdot \Delta \vec{r}_k ds' \quad (2)$$

With $\Delta \vec{r}_k = \vec{r}_k - \vec{r}_{k-1}$ and $\vec{r}_k = R_{MT} (\cos \frac{2\pi k}{N}, \sin \frac{2\pi k}{N})$ the vector pointing from the MT center to the k -th PF, cf. Fig 1. Equations 1-2 are 3-D analogues of the previously proposed stretchable railway-track [4] or wormlike-bundle [5] model for the case of a hollow circular bundle. While in general all the $N + 3$ fields, i.e. the 3 components of $\vec{\kappa}(s)$ and the PF displacements $\{u_k(s)\}_{k=1, \dots, N}$ enter the eqs 1-2 in the limit of small MT deviations from a straight line the problem can be drastically simplified. We first expand the tangent $\vec{t} \approx (\theta_x, \theta_y, 1)$ and $\vec{\kappa} \approx (\theta'_x, \theta'_y, 0)$ in terms of two angular projections θ_x and θ_y of \vec{t} in x and y direction respectively. Exploiting the circular geometry of the PF arrangement and the Fourier representation $u_k(s) = \sum \hat{u}_q(s) e^{\frac{2\pi i k q}{N}}$ over k we quickly realize that only the longest wavelength mode $\hat{u}_1(s)$ couples to overall MT backbone shape given by the curvature $\vec{\kappa}$. This leads to total energy decoupling $E_{MT} = E_{MT}^0 + E_{MT}^x + E_{MT}^y$ into a shape-independent

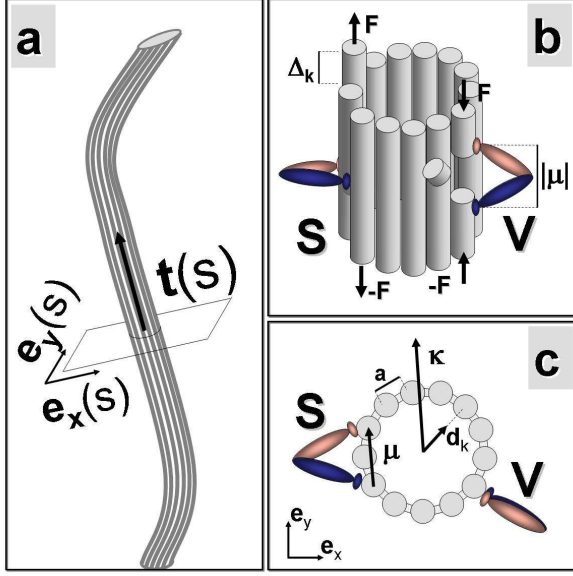


FIG. 1: (Color online) The basic geometry of motors inducing internal force doublets along the MT backbone: between two PFs (S-let) and along the same PF (V-let). The red and blue ovals represent two coupled motors or two motor sub-units (legs) of the same motor. Tubulin lattice vacancies at the motor position strongly amplify the MT backbone deformation (V^{gap} -let).

component E_{MT}^0 and two shape dependent contributions (in x and y direction) given by:

$$E_{MT}^i = \frac{1}{2} \int_{-L/2}^{L/2} \left[\hat{B} \Delta \theta_i'^2 + \hat{K}_c U_i'^2 + \hat{K}_s \hat{\Delta}_i^2 \right] ds \quad (3)$$

With $\hat{\Delta}_i(s) = a(\theta_i(s) - \theta_i(-L/2)) - U_i(s)$, $a = |\Delta \vec{r}_k|$ the inter-prot filament distance, $i = x, y$ and $\vec{U}(s) = (U_x, U_y) = (\text{Re} \chi \hat{u}_1, \text{Im} \chi \hat{u}_1)$ with $\chi = 1 - e^{-2\pi i/N}$ and renormalized constants $\hat{B} = NB$, $\hat{K}_c = NK_c / (4 - 4 \cos(2\pi/N))$ and $\hat{K}_s = NK_s$. Visually the new variable $\vec{U}(s)$ is a x-y vector at each MT-crosscut and can be interpreted as the (vectorial) mean over relative PF displacements of neighboring PFs. With this enormous simplification at hand we can consider now basic motor induced MT excitations (Fig 1). There are two elementary configurations in which motors can induce internal MT strains: 1) A motor (or a complex of several motors) acting between two (not necessarily neighboring) PFs and 2) A motor (or a complex of several motors) acting at two points within the same PF. For reasons that will soon become clear we call the excitation 1 S-type or simply an "S-let" and excitation 2 we call an V-type excitation or "V-let". Both excitations are "internal" in the sense that there is no net torque or force on the system motor+MT similarly to the case of a beating flagellum[1].

Elementary internal MT excitations. In the following we want to understand the properties of the two basic

types of excitations from Fig 1 and focus on the S-type first. We assume a single motor (or a complex of two motors) at position $s = s_0$ bridging between two PF with index k_1 and k_2 and exerting opposing forces F and $-F$ onto them respectively, Fig 1 a) (left) + b). The total energy is $E_{tot} = E_{MT} + E_{S-mot}$ with E_{MT} given by eqs 1-2 and the potential energy of the motor $E_{S-mot} = -F \sum_{k=k_1}^{k=k_2} \int_{-L/2}^{L/2} \delta(s - s_0) \Delta_k(s) ds$. As we had for E_{MT} before E_{S-mot} also decouples into independent modes in the Fourier representation over k and $E_{mot,S} = E_{S-mot}^0 + E_{S-mot}^x + E_{S-mot}^y$ with E_{S-mot}^0 a curvature independent term and the two shape dependent contributions $E_{S-mot}^{x/y}$ (in x and y direction) given by: $E_{S-mot}^i = -F \frac{\mu_i}{a} \int_{-L/2}^{L/2} \delta(s - s_0) \hat{\Delta}_i(s) ds$ with $i = x, y$ and $\vec{\mu}$ being the vector connecting the two attachment points of the motor (or motor complex) with components $\mu_i = \vec{\mu} \cdot \vec{e}_i$, Fig 1 b). The equilibrium solution is given by the Euler Lagrange equations: $\delta E_{tot}^i / \delta U_i = 0$ and $\delta E_{tot}^i / \delta \theta_i = 0$ with $E_{tot}^i = E_{S-mot}^i + E_{MT}^i$ and boundary conditions $\theta_i'(\pm L/2) = U_i'(\pm L/2) = 0$ (vanishing bending and shearing stresses at the ends). A short calculation leads to $\hat{\Delta}_i'' - \lambda^{-2} \hat{\Delta}_i = (1 + \alpha) \frac{\mu_i F}{a K_c} \delta(s - s_0)$ with the shear decay length $\lambda = (\lambda_c^{-2} + \lambda_B^{-2})^{-1/2}$.

Here the two important length scales $\lambda_c = \sqrt{\hat{K}_c / \hat{K}_s}$ and $\lambda_B = \sqrt{\hat{B} / a^2 \hat{K}_s}$ have the physical meaning of a pure compression- / pure bending- induced shear screening length respectively, with their squared ratio $\alpha = (\lambda_c / \lambda_B)^2 \approx 35$ ($N = 13$ PF). The remaining equations lead to conservation laws $(a\theta_i + \alpha U_i)' = 0$ which combined with the equation for $\hat{\Delta}_i$ give for the simplest symmetric case $s_0 = 0$ the tangent angles (up to an arbitrary constant)

$$\theta_i(s) = \Phi_i \frac{\cosh(|s|/\lambda - L/2\lambda)}{\sinh(L/2\lambda)} \quad (4)$$

With $\Phi_i = \Phi_i^S = \vec{\mu} \cdot \vec{e}_i \frac{\lambda F}{2B}$. The resulting MT backbone curvature has a jump at $s = 0$ and attains its maximal modulus there. The resulting MT shape is planar (contained in the plane spanned by $\vec{\mu}$ and \vec{t} at any position) and S-shape-like with initial and final angle coinciding $\theta_i(-L/2) = \theta_i(+L/2)$ which explains our nomenclature "S-type excitation" or "S-let". Interestingly the length scale λ over which $\theta_i(s)$ declines allows us to independently estimate the ratio of stretch and shear moduli from the observation of S-let deformations coming from katanin action[7], $Y/K_s \approx 64\pi^{-1} (\lambda/a)^2 \approx 6 \times 10^5$ for $\lambda \approx 1\mu m$ (cf, Fig 2b) and $a \approx 6nm$. This value is close to the result obtained by Pampaloni et al. [3] ($Y/K_s \approx 10^6$). Further the maximal deflection angle of $\theta_{max} \approx 38^\circ$ ($= 0.66$) measured in Fig 2a gives via 4 an estimate for the involved motor forces $F \approx 2\hat{B}\theta_{max}/(\lambda|\mu|) = \frac{13}{32}\pi a^4 Y / (\lambda|\mu|) = 20 - 250pN$ (for $|\mu| = a \approx 6nm$ and the range of values for Y from literature [2, 3]). This indi-

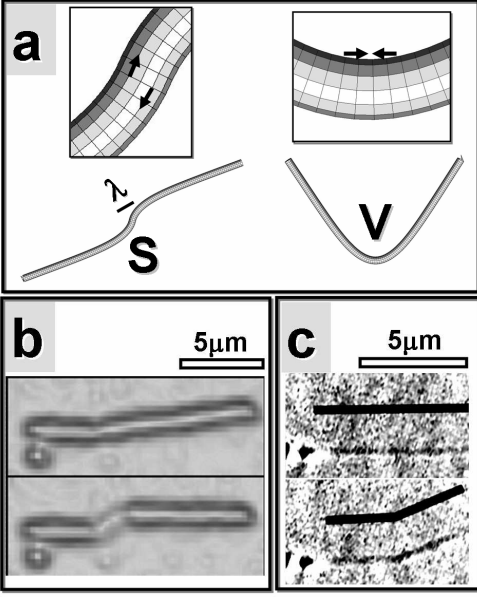


FIG. 2: a: The shapes of V and S-type excitations as given by Eq. 4 and their experimental observations for katanin operating on MTs (b,c). b: Adapted and edge enhanced image from [7]. c: Adapted from [6], black bars highlight the MT deformation. The upper and lower images show the MT before and after kink generation respectively.

cates that many katanin motors might act cooperatively to generate the observed shape change in Fig 2b. Another interesting possibility is that katanin might be different from dynein/kinesin by generating only small contractile displacement "powerstrokes" $\lesssim 1nm$ with a more efficient chemical-mechanical ATP-energy conversion leading to larger contractile forces $F \gtrsim 15k_B T/nm = 60 pN$.

The second fundamental internal MT excitation appears when a motor (or motor complex) acts along a single PF with index k compressing or stretching it. The motor energy in this case can be written as $E_{V,mot} = F(u_k(s_0 + |\mu|/2) - u_k(s_0 - |\mu|/2)) \approx F|\mu| \int_0^L \delta(s - s_0) u'_k(s) ds$ where $|\mu|$ is the size of the motor step. Like in the previous case it is sufficient to keep the energy contribution of the mode $q = 1$ as the others decouple from each other and from the curvature term. Along very similar line of derivation as in the S-type excitation case we obtain a solution which is planar and contained in the plane spanned by the vector \vec{r}_k and \vec{t} . The resulting tangent angles for an excitation in the middle of the MT ($s_0 = 0$) are given by eq 4 with $\Phi_i = \Phi_i^V(s) = \frac{s}{|s|} (\vec{e}_i \cdot \Delta \vec{r}_k) \frac{\gamma_i F |\mu|}{2(1+\alpha)B}$ which is now s dependent and changes sign at $s = 0$. Here $(\gamma_x, \gamma_y) = \sin(\pi/N)(1 - \cos(2\pi/N))^{-1} (\sin(2\pi(k+1/2)/N), -\cos(2\pi(k+1/2)/N))$. The resulting shape, that we call a "V-let", is a smooth V-shaped planar kink in the MT backbone with continuous curvature which relaxes on the length-scale λ . While su-

perificially similar the S-let and V-let solutions are physically very different for two reasons. First, the $s/|s|$ factor in the V-let solution changes the symmetry with respect to the S-let which leads to dramatic effects on the end-end distance as we see below. Second difference lies in the different scaling of the numerical prefactors which in the case of a V-let do not contain the screening length λ and involve additionally a very large reduction factor $1/(1+\alpha)$. In practice this suppresses significantly the involved deformations ($\theta \approx 10^{-5} - 10^{-6}$), orders of magnitude below that of a S-let corresponding to the same force ($\theta \approx 10^{-1}$). However the situation changes dramatically if the motor is operating at a position of a vacancy in the tubulin lattice, cf. Fig 1. In this case the motor is not hindered by the large rigidity of the short PF portion that the motor acts on. Formally there is no requirement of continuity for $u_k(s)$ of the involved PF k at the position of the gap. For such a combined defect + motor excitation which we call V^{gap} -let, the motor energy is given by $E_{V^{gap},mot} = F(u_k(s_0 + 0) - u_k(s_0 - 0))$ and its $U_{x/y}$ dependent component becomes $E_{V^{gap},mot}^i = F\gamma_i(U_i(s_0 + 0) - U_i(s_0 - 0))$. After a short calculation in direct analogy with the previous cases we obtain the same form as in eq 4 but with $\Phi_i = \Phi_i^{V^{gap}}(s) = \frac{s}{|s|} (\vec{e}_i \cdot \Delta \vec{r}_k) \frac{\lambda \gamma_i F}{B}$. While its functional form and symmetry coincide with that of the V-let, the prefactor of a V^{gap} -let solution is more similar in magnitude to that of a S-let. It is intuitive to think of a V^{gap} -let as a V-let with an effectively renormalized motor force $\bar{F} = 2a^{-1}\lambda(1+\alpha)F$. The distribution of angles of observed V-shapes measured by Davies et al [6] of $\theta_{max} \approx 15^\circ - 30^\circ$ (cf. Fig 2c) would suggest for the defect free case (V-let) a very large required force of $F = 6 \times 10^4 - 6 \times 10^5 pN$. However, the same estimate for the V^{gap} -let case gives much more moderate $10 - 100 pN$ (few tens of motors), showing the prime importance of lattice defects in the case of V type excitations. Interestingly Davies et al. [6] also suggested a crucial role of lattice defects based on the pattern and kinetics of MT decomposition by katanin.

Statistical mechanics of multiple excitations. It is particularly interesting to understand the collective contribution of a large number of internal MT excitations acting at random positions s_j and orientations $\vec{\mu}_j$ in addition to the MT thermal fluctuations. The motor energy for S- and V-lets becomes now respectively $E_{S,mot}^i = -\frac{F}{a} \sum_j \mu_j^i \hat{\Delta}_i(s_j)$ and $E_{V,mot}^i = -F \sum_j |\mu| \gamma_j^i U_i^i(s_j)$. It is convenient to introduce the vector $\vec{\mu}_{S/V,j}^i$ such that $\mu_{S,j}^i \equiv \mu_j^i$ and $\mu_{V,j}^i \equiv |\mu| \gamma_j^i$ ($i = x, y$). For a fixed (but arbitrary) distribution of motors the partition functions $Z_i = \int DU_i D\theta_i \exp(- (E_{MT}^i + E_{mot}^i)/k_B T)$ and the correlation functions $\langle \overline{\theta_{i,q} \theta_{i,p}} \rangle$ ($q, p \neq 0$) can be obtained. Here $\langle \dots \rangle$ denotes the average over the random motore distribution and $\overline{\dots}$ is the average over the thermal noise. $\langle \overline{\theta_{i,q} \theta_{i,p}} \rangle$ decomposes into the sum of a thermal contri-

bution $\langle \overline{\theta_{i,q}\theta_{i,p}} \rangle_T = 2k_B T L^{-1} G(q) \delta_{p,q}$ with the propagator $G(q) = \left(\hat{B}q^2 + \frac{q^2 \hat{K}_s a^2}{q^2 + \hat{K}_s / \hat{K}_c} \right)^{-1}$ and a motor contribution $\langle \overline{\theta_{i,q}\theta_{i,p}} \rangle_{S/V} = \Psi_{S/V}(p) \Psi_{S/V}(q) C_{S/V}(q, p)$. For S- and V-let case we have respectively $\Psi_S(p) = \frac{2F\hat{K}_c p^2}{L(\hat{K}_c p^2 + \hat{K}_s)} G(p)$ and $\Psi_V(p) = \frac{2Fa\hat{K}_s p}{L(\hat{K}_c p^2 + \hat{K}_s)} G(p)$, with the motor position and orientation correlator $C_{S/V}(q, p) = \left\langle \sum_{j,l}^N \mu_{S/V,j}^i \mu_{S/V,l}^i \cos(qs_j) \cos(psl) \right\rangle$. $C_{S/V}(q, p)$ is easily computed for the simplest choice of a uniform motor position and orientation distribution: $P(s_i) = 1/L$, $\vec{\mu}_{S/V,j} = |\mu_{S/V}| (\cos \phi_j, \sin \phi_j)$ with a random angle ϕ_j with a probability distribution $P(\phi_j) = 1/2\pi$. In this case we obtain the length reduction $\langle \overline{\Delta z} \rangle / L \approx \frac{1}{4} \sum_q \left(\langle \overline{\theta_{x,q}^2} \rangle + \langle \overline{\theta_{y,q}^2} \rangle \right)$ which naturally decomposes in a sum of a thermal fluctuation term and a motor term $\langle \overline{\Delta z} \rangle = \langle \overline{\Delta z} \rangle_T + \langle \overline{\Delta z} \rangle_{S/V}$. In the relevant limiting case $L/\lambda \gg 1$ we obtain for the thermal part

$$\frac{\langle \overline{\Delta z} \rangle_T}{L} \approx \frac{L}{6l_p^\infty} + \frac{1}{2} \sqrt{\frac{k_B T}{a^2 \hat{K}_s l_p^0}} \quad (5)$$

with the large and small scale persistence lengths given by $l_p^\infty = \left(\hat{B} + a^2 \hat{K}_c \right) / k_B T$ and $l_p^0 = (\alpha / (1 + \alpha))^{-3} \hat{B} / k_B T$. Interestingly the term $a^2 \hat{K}_s$ can be formally understood as an intrinsic self-tension straightening the MT at small scales. Similar formulas appear in different geometries for the railway-track[4] and wormlike-bundle model[5]. The motor dependent length reduction for the S-, V- and V^{gap} -let excitations with line density ρ is given by:

$$\frac{\langle \overline{\Delta z} \rangle_S}{L} = c_S \frac{\rho F^2 \mu^2}{a^4 \hat{K}_s^2 \lambda} \quad (6)$$

$$\frac{\langle \overline{\Delta z} \rangle_V}{L} = c_V \frac{\rho F^2 \mu^2 L}{a^2 \hat{K}_s^2 \lambda^4}, \quad \frac{\langle \overline{\Delta z} \rangle_{V^{gap}}}{L} = c_{V^{gap}} \frac{\rho F^2 \mu^2 L}{a^4 \hat{K}_s^2 \lambda^2} \quad (7)$$

with $c_S = \alpha^2 (1 + \alpha)^{-2} / 16 \approx 6 \times 10^{-2}$, $c_V = 0.18 \alpha^2 (1 + \alpha)^{-4} \approx 1.3 \times 10^{-4}$ and $c_{V^{gap}} = 0.73 \alpha^2 (1 + \alpha)^{-2} \approx 0.7$. Remarkably the S- and V/V^{gap} -lets show different scaling. In particular $\langle \overline{\Delta z} \rangle_{V/V^{gap}} / L$ grows with L (in analogy to the first term in the thermal contribution 5) while $\langle \overline{\Delta z} \rangle_S / L$ stays length independent. The physical reason for this difference becomes obvious from Fig 2, as the relative slack $\langle \overline{\Delta z} \rangle / L$ induced by a single S-let scales with λ/L , while for an V/V^{gap} -let it is essentially length independent. For longer MTs this effect leads to a strong dominance of V^{gap} -lets over S-lets $\langle \overline{\Delta z} \rangle_{V^{gap}} / \langle \overline{\Delta z} \rangle_S \sim (L/\lambda) \gg 1$. Although having the same L scaling the minute prefactor of defect free V-lets renders their contribution relatively insignificant $\langle \overline{\Delta z} \rangle_V / \langle \overline{\Delta z} \rangle_S \sim a^2 \lambda^{-3} L \approx 10^{-6}$ even for very

long MTs ($L = 100 \mu m$), underlining the importance of lattice vacancies transforming a V-let into a V^{gap} -let. Another interesting observation is that in all three cases $\langle \overline{\Delta z} \rangle_{S/V/V^{gap}} \propto \rho F^2$. Fixing the number of motors N_{mot} but regrouping them into N_{mot}/M clusters of size M we have $\rho \rightarrow M^{-1} \rho$, $F \rightarrow MF$ and therefore $\langle \overline{\Delta z} \rangle_{S/V/V^{gap}} \propto M$, i.e. the slack grows linearly with the cluster size. This indicates that cooperativity (positional correlation) of motor action can lead to strong enhancement of the slack length.

From Eqs.5-7 we can derive criteria for the dominance of motor slack over the thermal slack. For instance using the values estimated from Fig 2 b,c for katanin for elastic constants from [3] ($F = 20pN$, $\lambda = 1 \mu m$) and $\mu = 8nm$, $L = 20 \mu m$ we obtain $\langle \overline{\Delta z} \rangle / L = \rho / \rho_c$ with $\rho_{c,S} \approx 0.25 nm^{-1}$, $\rho_{c,V^{gap}} \approx 1.2 \times 10^{-3} nm^{-1}$. For large enough motor densities the katanin action easily dominates over the thermal slack $\langle \overline{\Delta z} \rangle_T / L \approx 6 \times 10^{-4}$.

Being evolutionary specialized for MT deformation and degradation katanin is likely to be among the strongest slack generating motors. We suspect however that classical motors like dynein and kinesin might cause less pronounced but observable effects as well. While dynein is known to walk between several PFs, kinesin is very strictly following a single one[1]. Our theory suggest that dynein should induce moving S-lets, yet with quickly fluctuating signs which would diminish the effect considerably. A battery of many kinesins, however, walking over a MT region with many tubulin vacancies, would give rise to spatially stationary V^{gap} -lets blinking between "on" and "off" states. The theoretical and experimental exploration of these issues is an interesting future direction.

The authors acknowledge fruitful discussions with E. Frey, C. Heussinger, M. Bathe, O. Campas, J.F. Joanny and P.C. Nelson. I.M.K. acknowledges support by the Max-Planck Society.

-
- [1] J. Howard, Mechanics of Motor Proteins and the Cytoskeleton. Sinauer Press (2001); L.A. Amos and W.G. Amos, Molecules of the Cytoskeleton, Guilford (1991).
 - [2] A. Kis et al. Phys. Rev. Lett. 89: 248101 (2002)
 - [3] F. Pampaloni et al. PNAS 103: 10248 (2006)
 - [4] R. Everaers, R. Bundschuh, and K. Kremer, Europhys. Lett 29, 263, (1995)
 - [5] C. Heussinger, M. Bathe and E. Frey, [cond-mat/0702097]
 - [6] L.J. Davis, D.J. Odde, S.M. Block, and S.P. Gross, Biophys. J. 82, 29162927 (2002)
 - [7] J.J. Hartmann et. al, Cell, Vol. 93, 277287; Movie at <http://valelab.ucsf.edu/images/mov-rhomtmsvkat.mov> with kind permission by R. Vale